Available online at www.sciencedirect.com
ScienceDirect
Journal of Photochemistry and Photobiology A: Chemistry 193 (2008) 266–270
Journal of Photochemistry and Photobiology A:Chemistry
www.elsevier.com/locate/jphotochem

Slurry photodegradation of 2,4-dichlorophenoxyacetic acid: A comparative study of impregnated and sol–gel In_2O_3–TiO_2 mixed oxide catalysts

V. Rodríguez-González [a], A. Moreno-Rodríguez [a], M. May [b], F. Tzompantzi [a], R. Gómez [a,*]

[a] *Universidad Autónoma Metropolitana-I, Depto. de Química, Av. San Rafael Atlixco No. 186, México 09340, D.F., Mexico*
[b] *Universidad Autónoma Metropolitana-A, Depto. de Química, Av. San Pablo No. 180, Col. Reynosa Tamaulipas 02200, D.F., Mexico*

Received 16 January 2007; received in revised form 23 June 2007; accepted 7 July 2007
Available online 12 July 2007

Abstract

The synthesis, characterization and photocatalytic properties of impregnated In_2O_3/TiO_2 and In_2O_3–TiO_2 sol–gel catalysts were reported. A specific surface area was obtained on the In_2O_3–TiO_2 catalysts prepared by the sol–gel method (153 m^2/g) which was three times higher than that on the In_2O_3/TiO_2 impregnated catalysts (58 m^2/g). The XRD spectra of the samples showed the anatase phase as the only crystalline phase present in both catalysts. The determination of the E_g band gap by UV–vis spectroscopy showed a band gap of 3.5 eV for the In_2O_3–TiO_2 photocatalysts while for the In_2O_3/TiO_2 samples it was of 3.1 eV. The obtained photoactivity for the 2,4-dichlorophenoxyacetic acid degradation by the In_2O_3–TiO_2 sol–gel catalysts ($t_{1/2}$ = 35 min) was higher than the obtained by the In_2O_3/TiO_2 impregnated catalysts ($t_{1/2}$ = 88). The higher activity showed by the sol–gel photocatalysts can be related with specific surface area effects combined with those produced by the formation of highly dispersed In_2O_3 particles; and by the insertion of some In^{3+} cations in the titania framework.

Keywords: Indium oxide photocatalysts; 2,4-Dichlorophenoxyacetic acid degradation; Indium–titania mixed oxide XRD; Indium–titania mixed oxide; Sol–gel photocatalysts; Indium–titania mixed oxide Raman; Indium–titania mixed oxide UV–vis

1. Introduction

The photocatalytic degradation of pollutants in water has been successfully carried out by using suspensions of powdered TiO_2 semiconductors [1–3]. Titania has attracted the attention of many scientists and its preparation has been carried out by using several techniques [4–11]. Particularly, the preparation of titanium dioxide by the sol–gel method has been reported as one of the most promising methods to obtain high active photocatalysts. The sol–gel method permits the modification of the textural, structural and semiconductive properties of the material. Additionally, it allows the possibility of doping the semiconductor with several cations during the gelling step [12–16].

A different method to prepare efficient photocatalytic titania is by coupling it with other semiconductor oxides, such as In_2O_3 [17–19]. By doping titania with semiconductors, structural modifications in the titania framework are obtained when Ti–O–M–O bonds are formed.

Indium oxide has been extensively reported as one of the most interesting semiconductors and its band gap is 3.7 eV [19,20] and a great number of applications have been reported, for example, in the development of solar cells [21], photovoltaic and optoelectronic devices [22]; and liquid crystal displays [23,24]. However, as photocatalyst, In_2O_3 has been scarcely reported [18].

By taking into account the aforementioned, in the present work, indium oxide was chosen as the coupled oxide for TiO_2. The In_2O_3–TiO_2 photocatalyst was prepared by the sol–gel method, by using indium acetylacetonate and titanium alkoxides as sol–gel precursors. The photocatalytic properties of the sol–gel catalyst were evaluated in the 2,4-dichlorophenoxyacetic acid (2,4-D) degradation and compared with the activity of an In_2O_3/TiO_2 impregnated photocatalyst.

* Corresponding author.
E-mail addresses: vrg@xanum.uam.mx (V. Rodríguez-González), albinomx@yahoo.com (A. Moreno-Rodríguez), may@correo.azc.uam.mx (M. May), fjtz@xanum.uam.mx (F. Tzompantzi), gomr@xanum.uam.mx (R. Gómez).

1010-6030/$ – see front matter © 2007 Elsevier B.V. All rights reserved.
doi:10.1016/j.jphotochem.2007.07.005

2. Experimental

2.1. Catalysts preparation

The sol–gel In_2O_3–TiO_2 mixed oxides were prepared by using titanium(IV) butoxide (Aldrich 97%) and indium acetylacetonate (Chemat 98%) as precursors. A solution containing indium acetylacetonate–acetone and 63 mL of titanium butoxide were simultaneously added to a solution containing 115 mL of distilled water and 190 mL of *n*-butanol. Then, the solution was maintained under reflux for 48 h until gelling. Afterwards, the sample was dried in air at 70 °C for 12 h and then calcined at 500 °C for 4 h by using a programmed heating rate of 2 °C/min. The quantity of indium acetylacetonate co-gelled with the titanium alkoxide was calculated to provide 12 wt% of indium oxide in the titanium dioxide. The impregnated In_2O_3/TiO_2 photocatalyst was prepared by incipient impregnation with indium acetylacetonate–acetone (12 wt% In_2O_3) of sol–gel titania which was previously calcined at 500 °C. The reference In_2O_3/P25 was prepared by impregnation with indium acetylacetonate–acetone of commercial P25 titania which was previously treated in air at 500 °C for 4 h.

2.2. Catalysts characterizations

The specific surface areas were calculated from the nitrogen adsorption isotherms by the BET method, by using an Autosorb-3B automatic apparatus (Quantachrome Corporation). The pore size distribution was calculated from the desorption isotherm by using the BJH method.

The crystalline phase was determined by X-ray diffraction with a Bruker D-8 Diffractometer by using Cu Kα radiation. The UV–vis spectra (200–900 nm) of the solids were obtained with a UV–vis Varian spectrophotometer, model Cary 100 (diffuse reflectance). The E_g band gap was calculated by extrapolation of the UV band to the *x*-axis for $y = 0$ [16].The Raman spectra were recorded on a Nicolet Almega Dispersive Raman Spectrometer, equipped with a $NdYVO_4$ laser source. The laser excitation line was 532 nm and the power was of 25 mW.

2.3. Photocatalytic activity

The photocatalytic degradation was performed with UV light irradiation in a slurry reactor at room temperature. The used UV source was a standard Pen-Ray lamp (UVP Products Cat. No. 90-0012-01) with a typical λ intensity of 254 of 4400 μW/cm^2. The quartz lamp was immersed in a cooled vessel containing the reactant solution consisting of 100 mL with 40 ppm (1.8×10^{-4} M) of 2,4-dichlorophenoxyacetic acid and 100 mg of catalyst. In order to achieve the saturation of dissolved oxygen and assure the adsorption of the 2,4-D molecule on the semiconductor, a flux of dry air was bubbled for 30 min (1 mL/s) before turning on the light source. The photo-degradation was monitored with a UV–vis Varian spectrophotometer, model Cary 100 by following the main 2,4-D absorption band at 229 nm as a function of the irradiation time.

3. Results and discussion

The nitrogen adsorption–desorption isotherms of the various samples are showed in Fig. 1. As for the TiO_2 and In_2O_3–TiO_2 sol–gel catalysts, the isotherm form corresponds to that of type 5 in the BDDT classification; and the type E hysteresis loop is in agreement with the De Boer classification attributed to mesoporous solids [25]. On the other hand, the pore size distribution for the materials is presented in Fig. 2, where a narrow pore size distribution can be seen for the sol–gel preparations. The calculated specific surface areas and mean pore size diameter reported in Table 1 showed that the highest specific surface area corresponds to that of the In_2O_3–TiO_2 sol–gel mixed oxide (153 m^2/g). Thus, when the titanium alkoxide and indium acetylacetonate were co-gelled, a positive effect on the textural

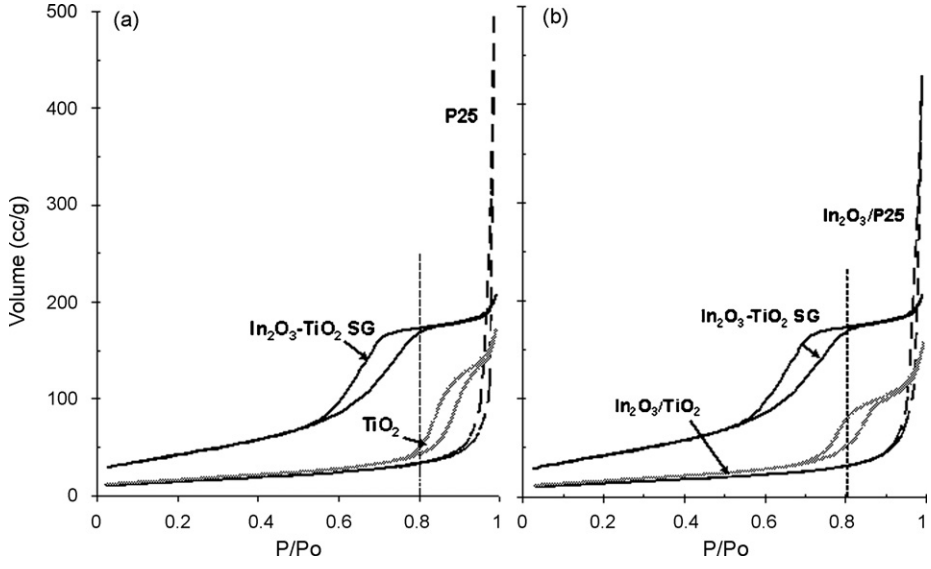

Fig. 1. Nitrogen adsorption isotherms for (a) P25, TiO_2, In_2O_3–TiO_2 sol–gel and (b) impregnated catalysts.

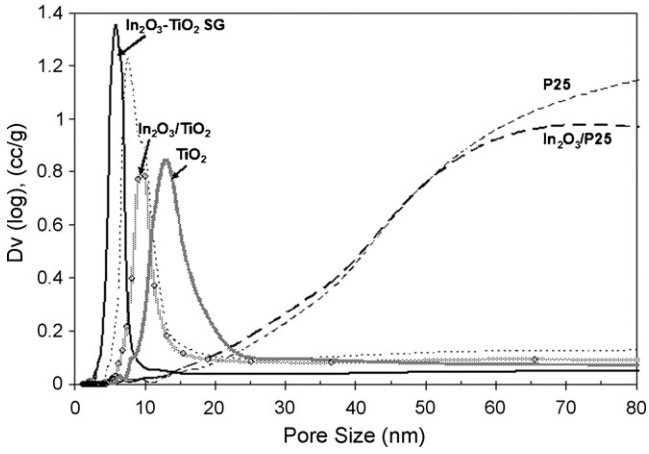

Fig. 2. Pore size distribution for P25, TiO_2, In_2O_3–TiO_2 sol–gel and impregnated catalysts.

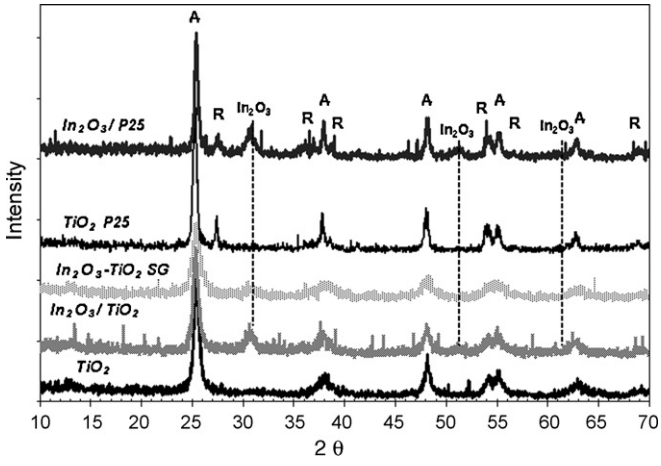

Fig. 3. XRD patterns for P25, TiO_2, In_2O_3–TiO_2 sol–gel and impregnated catalysts. A: anatase, R: rutile.

properties of the mixed oxide was obtained. As for the TiO_2 and impregnated In_2O_3/TiO_2 catalysts, the BET specific surface areas were 65 and 58 m^2/g, respectively. A small pore size diameter (7 nm) was obtained for the In_2O_3–TiO_2 mixed oxide, while the mean pore size diameters for the TiO_2 and In_2O_3/TiO_2 were of 13 and 9 nm, respectively. Concerning the Degussa P25 titanium oxide, the BET specific surface area is reported as an illustrative value.

The XRD patterns for the In_2O_3–TiO_2 sol–gel catalysts and TiO_2 showed anatase as the crystalline phase (Fig. 3). As for titania P25, the XRD characteristic peaks of anatase and rutile are clearly observed. The diffractogram signals corresponding to indium oxide are observed in the impregnated samples ($2\theta = 31.2$). As for the In_2O_3–TiO_2 sol–gel catalyst, the corresponding signal to indium oxide decreases remarkably and a very small peak can be seen. The insertion of some In^{3+} in the titania framework which forms either O–Ti–O–In–O bonds or highly dispersed In_2O_3 particles over TiO_2 is certainly the responsible of the small indium oxide XRD detection. The amount of In_2O_3 in the sol–gel mixed oxide was 12 wt%; hence, by XRD spectroscopy it was expected that the corresponding signal should have been observed of the same intensity as it is showed in the impregnated samples.

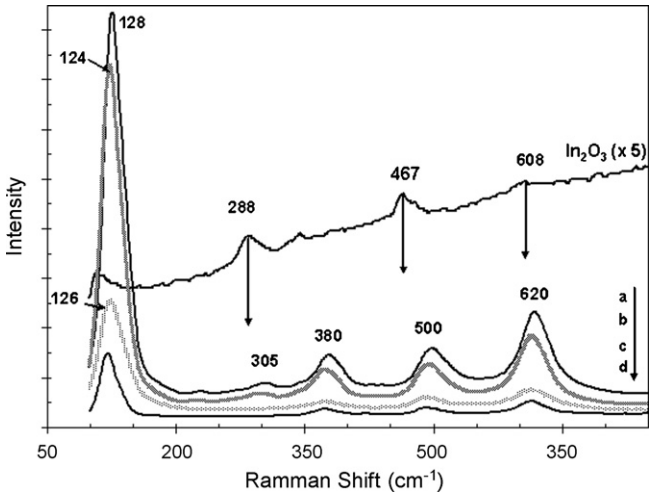

Fig. 4. Raman spectra for (a) TiO_2 sol–gel, (b) TiO_2–In_2O_3, (c) In_2O_3/P25 and (d) In_2O_3/TiO_2 catalysts.

The Raman spectra of the TiO_2, In_2O_3–TiO_2, In_2O_3/P25, In_2O_3/TiO_2 and indium acetylacetonate, which were calcined at 600 °C, are shown in Fig. 4. A shift in the E1g signal at 124 cm^{-1} for the anatase to 128 cm^{-1} in the In_2O_3–TiO_2 mixed oxide can be seen. Although this could be attributed to a change in the particle size, the shift of the position band of the E1g signal of the anatase signal was recently reported as an effect due to the insertion of In_2O_3 into the TiO_2 framework [26].

The E_g band gap was calculated from the UV–vis absorption spectra and the values are reported in Table 1. As for the P25 and TiO_2 bare samples, the E_g values are in the same order (3.3 and 3.1 eV), meanwhile, a higher value (3.5 eV) in the In_2O_3–TiO_2 sol–gel mixed oxide was obtained. The reported E_g band gap

Table 1
Specific surface area (S_{BET}), band gap (E_g) and photocatalytic activity ($t_{1/2}$) for the 2,4-dichlorophenoxyacetic acid degradation over In_2O_3–TiO_2 sol–gel prepared mixed oxides and impregnated photocatalysts

Catalyst	S_{BET} (m^2 g^{-1})	Pore size (nm)	E_g (eV)	$t_{1/2}$ (min)	% C[a]	k[b] (min^{-1})	k/S_{BET} ($\times 10^3$ min^{-1} m^{-2} g)
P25	54	–	3.3	100	60	0.0067	1.24
TiO_2	65	13	3.1	90	69	0.0085	1.30
In_2O_3–TiO_2 SG	153	7	3.5	35	95	0.0208	1.36
In_2O_3/TiO_2	58	9	3.1	88	69	0.0075	1.29
In_2O_3/P25	48	–	2.8	154	57	0.0058	1.20

[a] $t = 180$ min.
[b] From Fig. 9.

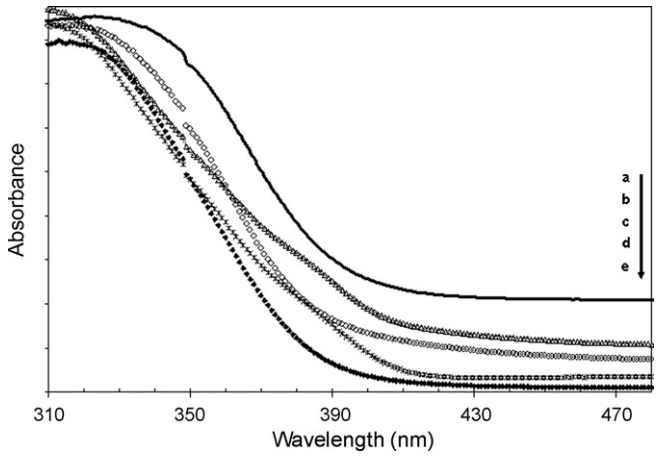

Fig. 5. UV–vis spectra for the semiconductors: (a) TiO_2 sol–gel, (b) In_2O_3/P25, (c) In_2O_3/TiO_2 sol–gel, (d) TiO_2 P25 and (e) In_2O_3–TiO_2 catalysts.

for thin films of In_2O_3 was 3.7 eV [19,20]; then a medium value between the anatase and In_2O_3 was obtained in the mixed oxide. On the impregnated samples, the E_g values were 3.1 and 2.8 eV for the In_2O_3/TiO_2 and In_2O_3/P25 supported catalysts, respectively. The effect on the band gap energy depends on the method used to incorporate the indium acetylacetonate precursor (impregnation or sol–gel). As for the sol–gel In_2O_3–TiO_2 mixed oxide, the doping of the titania network can exert a direct effect on the conduction band. A similar effect has been observed on the TiO_2 thin films, where an increase in the band gap as a function of the In_2O_3 concentration was reported [27]. On the other hand, concerning the impregnated catalysts, the effect must be similar to that extensively reported for metal oxides deposited over TiO_2, in which the role of the supported oxide is related to a decrease in the electron–hole recombination [2–4]. In Fig. 5, the UV spectra for all the samples are illustrated.

The evolution of the 2,4-dichlorophenoxyacetic acid as a function of time is illustrated in Fig. 6, where it can be seen that the degradation of the 2,4-D can be evaluated with accuracy by following the 229 nm absorption band. On the other hand, the photolysis and adsorption in dark of the 2,4-D are presented

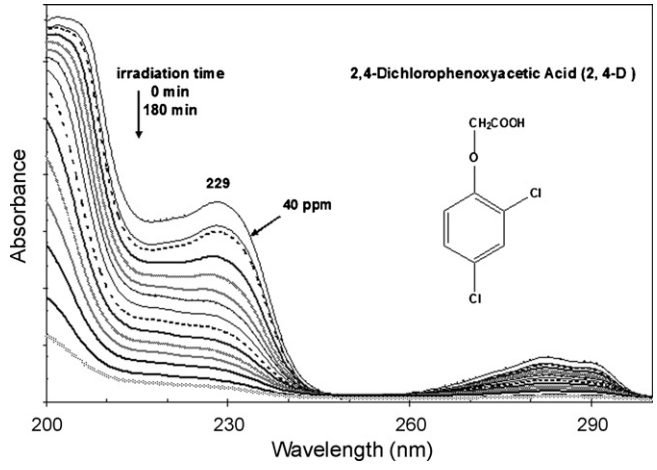

Fig. 6. UV–vis absorption spectra evolution as a function of time for the 2,4-D photodecomposition over TiO_2–In_2O_3 sol–gel prepared catalyst.

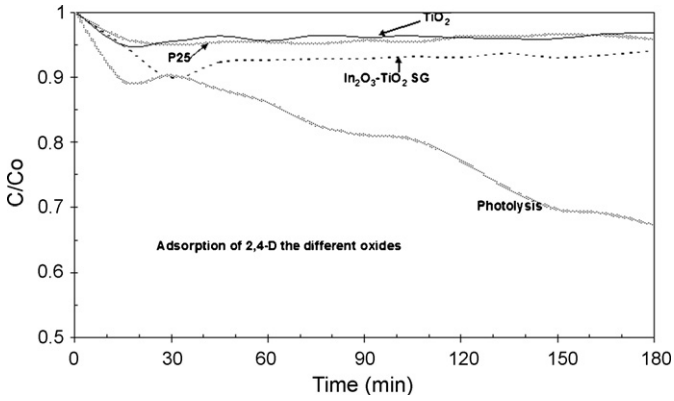

Fig. 7. Adsorption in dark and photolysis under UV light for the 2,4-dichlorophenoxyacetic acid as a function of time.

in Fig. 7. Even when the photolysis with a UV light source is important (25%), the 2,4-D does not disappear after 180 min under irradiation.

The photocatalytic degradation of the 2,4-D as a function of time is showed in Fig. 8; and the corresponding activities were reported as $t_{1/2}$ in Table 1. The lowest activities correspond to the In_2O_3/P25 and P25 catalysts ($t_{1/2}$ of 154 and 100 min, respectively). As for TiO_2, the $t_{1/2}$ was of 90 min and slightly diminishes in the impregnated In_2O_3/TiO_2 catalyst ($t_{1/2}$ = 88 min). However, when the catalyst was prepared by co-gelling aluminium alkoxide and indium acetylacetonate, the obtained In_2O_3–TiO_2 mixed oxide showed the highest photoactivity, $t_{1/2}$ = 35 min, Table 1. Such results show that the impregnation with a semiconductor is not enough to improve the photocatalytic properties.

All the catalysts followed pseudo-first-order kinetics and the apparent rate constant was calculated by plotting ln (C_0/C) versus time (Fig. 9). The slope of the plot represents the apparent rate constant. The highest rate constant for the degradation was obtained in the In_2O_3–TiO_2 catalyst (Table 1).

The photoactivity enhancement obtained on the In_2O_3–TiO_2 sol–gel photocatalyst certainly resides in the preparation method. We assume that some In^{3+} cations are substituting

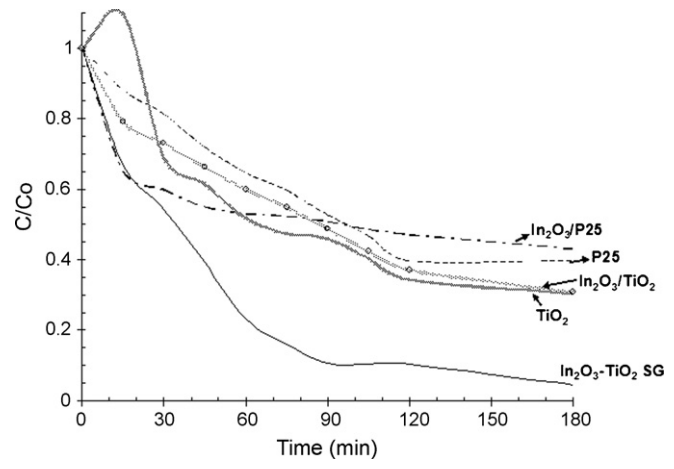

Fig. 8. Photocatalytic degradation for 2,4-dichlorophenoxyacetic acid as a function of time.

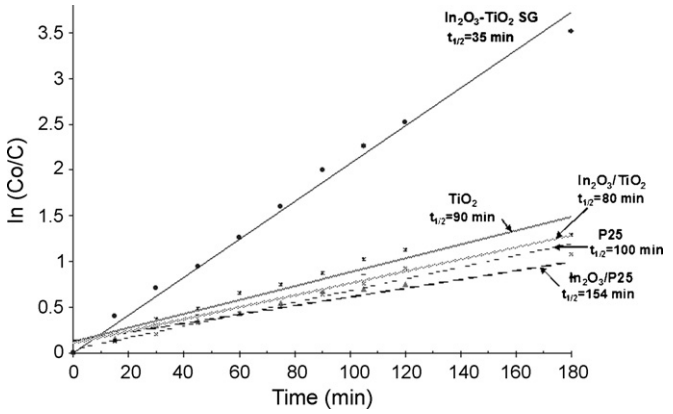

Fig. 9. Pseudo-first-order kinetics and apparent rate constant for the 2,4-dichlorophenoxyacetic acid degradation.

Ti^{4+} cations in the titania framework by forming Ti–O–In–O–Ti bonds; however, the identification of such species is very difficult. Firstly, only few In^{3+} species can be inserted in the titania framework, and the In^{3+} ratio is 94 pm (hexacoordinated), which compared with the Ti^{4+} ratio of 74.5 pm (hexacoordinated) is too high to expect a large substitution. The difficulty to identify the substitution is obvious; however, the shift in the Raman signal showed in Fig. 4 can be used as a good support to our assumption.

The effect of the specific surface area on the activity was analyzed and the 2,4-D decomposition per m^2, which was expressed as k/S_{BET} is of the same order in both, the sol–gel In_2O_3–TiO_2 and In_2O_3/TiO_2 photocatalysts (Table 1). However, in Fig. 8, it can be seen that only the mixed oxide practically decomposes all the herbicide after 150 min (95% C). As for the impregnated In_2O_3/TiO_2 catalysts as well as the reference supports, the reaction seems to reach the equilibrium where the total 2,4-D degradation was not achieved. The 2,4-D decomposition after 180 min was of 60 % and 69% C for the reference supports and 69 and 57% C for both the In_2O_3 impregnated on TiO_2 and P25 catalysts, respectively. This behaviour showed that only the In_2O_3–TiO_2 mixed oxide is able to destroy practically the whole 2,4-D contained in the reactant solution. On the other catalysts the formation of by-products inhibits the 2,4-D decomposition. The identification of the by-products is in course and they will be the subject of a coming publication.

4. Conclusions

It is proposed that some In^{3+} cations are inserted in the titania framework during the sol–gel preparation and produce important effects on the specific surface area; and hence, on the photocatalytic properties. However, at the same time, indium oxide presented small clusters over the support which played the role of electron captors and produced a better separation of the photogenerated charge in the carriers. The advantage of the sol–gel method [28] to synthesize mixed oxides is that the formation of highly dispersed In_2O_3 particles and In^{3+} doping effects could be present at the same time in the In_2O_3–TiO_2 sol–gel photocatalysts. As a result of the combination of both effects, an important photoactivity improvement was obtained.

Acknowledgements

V.R.G. thanks CONACYT-México for the Postdoctoral research fellowship. The authors want to thank G. Mendoza for his technical support.

References

[1] O.M. Alfano, D. Bahnemann, A.E. Cassano, R. Dillert, R. Goslich, Catal. Today 58 (2000) 199.
[2] J.M. Herrmann, Catal. Today 53 (1999) 115.
[3] M. Anpo, Pure Appl. Chem. 72 (2000) 1265.
[4] M.I. Litter, Appl. Catal. B: Environ. 23 (1999) 89.
[5] K. Wilke, H.D. Breuer, J. Photochem. Photobiol. A 121 (1999) 49.
[6] I. Justicia, G. Garcia, L. Vazquez, J. Santiso, P. Ordejon, G. Basttiston, R. Gerbasi, A. Figueras, Sens. Actuator B: Chem. 109 (2005) 52.
[7] A. Fujishima, T.N. Rao, D.A. Tryk, J. Photochem. Photobiol. C: Photochem. Rev. 1 (2000) 1.
[8] C. Chen, X. Li, W. Ma, J. Zhao, H. Hidaka, N. Serpone, J. Phys. Chem. B 106 (2002) 318.
[9] N. Negishi, K. Takeuchi, T. Ibusuki, J. Sol–Gel Sci. Technol. 13 (1998) 691.
[10] N. Negishi, K. Takeuchi, J. Sol–Gel Sci. Technol. 22 (2001) 23.
[11] N. Smirniova, A. Eremenko, V. Gayvoronskij, I. Petrik, Y. Gnatyuk, G. Krylova, A. Korchev, A. Chuiko, J. Sol–Gel Sci. Technol. 32 (2004) 357.
[12] J.C.S. Wu, C.H. Chen, J. Photochem. Photobiol. A 163 (2004) 509.
[13] A. Piscopo, D. Robert, J.V. Weber, J. Photochem. Photobiol. A 139 (2001) 253.
[14] T. Lopez, R. Gomez, E. Sanchez, F. Tzompantzi, L. Vera, J. Sol–Gel Sci. Technol. 22 (2001) 99.
[15] T. Lopez, J. Hernandez-Ventura, R. Gomez, F. Tzompantzi, E. Sanchez, X. Bokhimi, A. Garcia, J. Mol. Catal. A: Chem. 167 (2001) 101.
[16] R. Gomez, T. Lopez, E. Ortiz-Islas, J. Navarrete, E. Sanchez, F. Tzompantzi, X. Bokhimi, J. Mol. Catal A: Chem. 193 (2003) 217.
[17] W.A. Badawy, J. Mater. Sci. 32 (1997) 4979.
[18] D. Shchukin, S. Poznyak, A. Kulak, P. Pichat, J. Photochem. Photobiol. A 162 (2004) 423.
[19] S.K. Poznyak, D.V. Talapin, A.I. Kulak, J. Phys. Chem. B 105 (2001) 4816.
[20] L. Gupa, A. Mansingh, P.K. Srivastsva, Thin Solid Films 176 (1989) 33.
[21] O.N. Srivastava, R.K. Karn, M. Misra, Int. J. Hydrogen Energy 25 (2000) 495.
[22] C.G. Granqvist, Appl. Phys. A57 (1993) 19–24.
[23] K.G. Gopchandran, B. Joseph, J.T. Abraham, P. Koshy, V.K. Vaidyan, Vacuum 86 (1997) 547.
[24] N.N. Greenwood, A. Earnshaw, Chemistry of the Elements, 2nd ed., Elsevier, 1998, p. 222.
[25] J.H. de Boer, The Structure and Properties of Porous Materials, Butterworths, London, 1958, p. 68.
[26] M.A. Debeila, R.P.K. Wells, J.A. Anderson, J. Catal. 239 (2006) 162.
[27] K.S. Chandra Babu, D. Singh, O.N. Srivastava, Int. J. Hydrogen Energy 16 (1991) 387.
[28] X. Bokhimi, A. Morales, O. Novaro, T. Lopez, E. Sanchez, R. Gomez, J. Mater. Sci. 10 (1995) 2788.